Cross-section of electrical impact excitation in bulk n-type monocrystalline Al:Cr:ZnSe

OZARFAR GAFAROV,* RICK WATKINS, VLADIMIR FEDOROV, AND SERGEY MIROV

Department of Physics, University of Alabama at Birmingham, CH 310, 1300 University Blvd., Birmingham, AL 35294, USA
*ozarfar@uab.edu

Abstract: Middle-infrared luminescence of bulk Al:Cr:ZnSe crystal under direct electrical excitation of $Cr^{2+}, {}^5E- {}^5T_2$ transition, is reported. Effective cross-section of electrical excitation was estimated based on comparative luminescence measurements under electrical and optical (1560 nm) excitations. Calculation of the threshold current density for lasing under electrical excitation of this material was also performed.

1. Introduction

In the recent decades, middle-Infrared (mid-IR) broadly tunable lasers based on Transition Metal (TM) doped II-VI chalcogenides, such as Cr(Fe):ZnSe and Cr(Fe):ZnS, have been intensively studied. The reason for such a strong interest in these materials stems from their unique combination of favorable characteristics including wide mid-IR transparency window, broad absorption and emission bands, high cross-sections of absorption and emission, absence of the excited state absorption, and wide-bandgap. A considerable progress in TM:II-VI laser characteristics has been achieved. For instance, high output power over 140 W, 1.6 J output energy, narrow (<100 kHz) linewidth, and sub-two cycle fs-pulses (15 fs) have been demonstrated [1–3]. The entirety of these results was achieved utilizing optical pumping. Due to the semiconductor nature of these materials, they hold potential for direct electrical pumping, however, no lasing under electrical excitation has been documented in the literature. Electrically pumped lasers based on TM:II-VI materials would be ideal for compact and cost-effective mid-IR lasers. The devices based on impact excitation under high electric field feature a straightforward design and have been demonstrated in several publications (see [4–10] and references therein). Cathodoluminescence of Cr:ZnS, where Cr^{2+} ions are excited by an energetic electron beam, was reported in [5]. Electroluminescence (EL) of a similar system, Fe:InP, was demonstrated by Scamarcio et al. [6]. First studies of mid-IR EL of Cr^{2+} in bulk polycrystalline ZnSe were performed by our group [4,7], while EL in bulk Cr:ZnSe single crystals [8,9] was reported soon after. However, a low electro-optical conversion ratio of ~10^{-6} was observed in both cases. Although readily available, polycrystalline samples have a drawback associated with a high probability of electrical shortening through the grain boundaries, where aggregation of metal ions can be present. The low yield in monocrystalline Cr:ZnSe was attributed to poor carrier injection in the metal-semiconductor interface by the authors [9]. Despite the simple design, demonstration of lasing of Cr:ZnSe/ZnS devices under electrical impact excitation requires a fine optimization of optical and electrical properties of the monocrystalline laser media, such as Cr^{2+} concentration, low losses in mid-IR, appropriate conductivity level, and formation of Ohmic contacts. This work is focused on the optimization of the optical and electrical properties of bulk monocrystalline Al:Cr:ZnSe and direct comparison of mid-IR EL and photoluminescence (PL) at ${}^5T_2 \rightarrow {}^5E$ transition of Cr^{2+} ions with a goal of calculation of the cross-section of electrical excitation and estimation of the threshold current density required for achieving lasing under electrical impact excitation.

2.   Sample preparation and experimental setup

Monocrystalline ZnSe samples were used in these experiments. All samples were cleaned in a sonic bath with Acetone, Methanol, 0.5 M HCl, 0.5 M NaOH, and deionized water, in the listed sequence, before being thermal diffusion doped. The samples were initially doped with Cr according to a well-established procedure that enables controlled doping of ZnSe to the desired Cr concentration [11]. Next, the samples were doped with Al. Aluminum doping can be carried out in multiple ways, from the gas phase of Al, the liquid phase of Al, or liquid phase of Al and Zn mix [12–16]. The low vapor pressure of Al at 1000° C provides conductivity only in a thin layer that can be easily eliminated by slight surface polishing. A more robust technique is annealing in contact with Al or Al/Zn mix. The latter provides a better conductivity, which is consistent with the improvement of diffusion of TM ions in the presence of Zn vapor reported in [17]. Moreover, interstitial Zn is known to provide n-type carriers in this system. The n-type doping of our crystals was facilitated by placing Cr:ZnSe and pieces of Zn and Al (200 mg and 10 mg, respectively) together and tightly wrapping with Molybdenum foil. The wrapping ensures a close contact between the Cr:ZnSe and Al/Zn melt throughout duration of annealing (16-100 hours) at 1000° C in evacuated (10^{-3} Torr) quartz ampules. The variation in annealing times was used as the means for controlling the carrier concentration. Under this variation different resistivity levels were reached, ranging from ∼50 Ωcm to ∼54 kΩcm. The best electrical conductivity was demonstrated by annealing ZnSe in Zn + Al (0.5-1.0%) melt. The dependence of electrical conductivity on Al concentration in the samples is complicated due to a strong self-compensation effect in ZnSe samples [18]. The total Al concentrations in the fabricated samples were not measured, while carrier concentrations were estimated using electron mobility at RT $\mu_e \approx 200$ cm^2/Vs [18]. The XRD measurements did not reveal any significant modification of the crystalline structure of the tested samples after annealing. A more detailed characterization of the influence of the chromium and aluminum concentration on the lattice parameters is underway. The concentrations of Cr^{2+} ions in the ZnSe samples were estimated using values of the absorption cross-section for the $^5T_2 \rightarrow ^5E$ transition equal σ=1.1×10^{18} cm^2 at 1.77 μm [1]. The Cr^{2+} absorption spectra measured before and after annealing in Al and Zn melt are shown in Fig. 1, where it can be seen that the Cr^{2+} absorption decreased by ∼1.6 times after the Al doping. This decrease can be attributed to the solvent extraction process, which relies on higher solubility of a solute in liquid solvent as compared to a solid solvent. The ratio of the solubility in solid over the solubility in liquid, when the two form an interface, is ∼3 orders of magnitude larger in liquid Zn than in solid ZnSe, for certain TM ions, at 950° C [19].
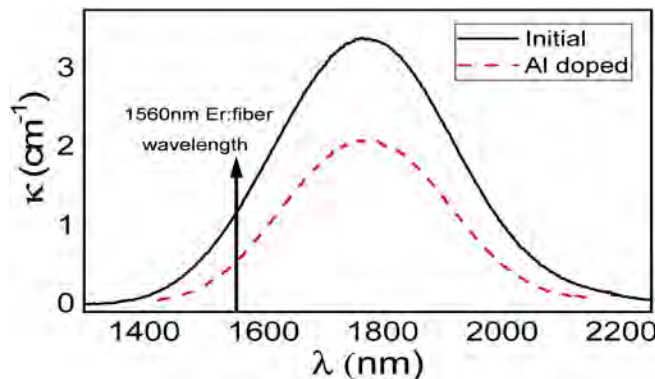
Fig. 1. Cr:ZnSe absorption spectra before (solid) and after (dashed line) Al/Zn doping.

As was mentioned above, lasing of Cr:ZnSe/ZnS devices under electrical impact excitation requires fine optimization of optical and electrical properties of the gain media as well as formation of Ohmic contacts. Ohmic contacts are achieved when the Schottky barrier, formed on the metal-semiconductor interface is minimized, i.e., electrons can cross the barrier under small forward bias voltages. The two main models that describe the Schottky barrier formation are the Schottky and the Bardeen models. The latter model predicts that the density of the surface states determines the height of the Schottky barrier. Authors in [20] demonstrated that for the more ionic II-VI materials like ZnSe the effect of the surface states is negligible. Thus, considering the classical Schottky model is sufficient to predict the barrier height. According to this model, the barrier height - $\Phi_B = \Phi_m - X_S$, where Φ_m - the metal work function and X_S - the electron affinity of the semiconductor material. The electron affinity of ZnSe is 4.09 eV [21]. Aluminum, Chromium, and Iron have metal work functions of 4.28 eV, 4.50 eV, and 4.50 eV, respectively [22]. Thus, these metals were chosen as suitable candidates. To fabricate Ohmic contacts, a 50 nm metal film was deposited on crystal facets and annealed at 900° C for three hours. The short annealing period preserves significant thickness of the metal film on the surface while highly doping a small depth in semiconductor. This method is extensively used for formation of Ohmic contacts. An additional 200 nm silver film was deposited as a protective layer, afterward. The best results for Al:ZnSe samples were seen for Cr-Ag and Fe-Ag contacts. Figure 2. – A shows I – V characteristics of the n-type Al:ZnSe samples with Cr-Ag, and Fe-Ag contacts, which exhibit consistent resistivities of 1.9 and 2.6 kΩcm, respectively. Ohmic behavior can be seen in the figure for both Cr-Ag and Fe-Ag metal contacts. On the other hand, contacts based on Al had very strong contact resistance, not shown in the figure. This failure can be attributed to the Aluminum's oxidation tendency. A second method for the formation of Ohmic contacts after Al doping, for n-type conductivity, was used. This method is simpler and consists of "ironing" Indium onto crystal facets until wetting and adhesion of Indium onto the crystal occurs [23]. After coating two parallel facets, the samples are heated at 250-300° C for ~1 minute in the ambient atmosphere. The formation of Ohmic contacts, in this method, takes place during the cool down process after being heated according to [23]. Although quick and straightforward this method is hard to use on samples < 0.5 mm in thickness. The electrical characteristics of an Al:Cr:ZnSe (sample #1, $N_{Cr} \approx 2{\times}10^{18}$ cm^3) with dimensions of ~2.6×2.6×1.2 mm^3, which had "ironed"-on Indium contacts, is shown in Fig. 2 – (B). No Schottky barrier was observed at low values of applied voltages. A quasi-Ohmic behavior was observed, with a pure Ohmic behavior for voltages < 100 V.
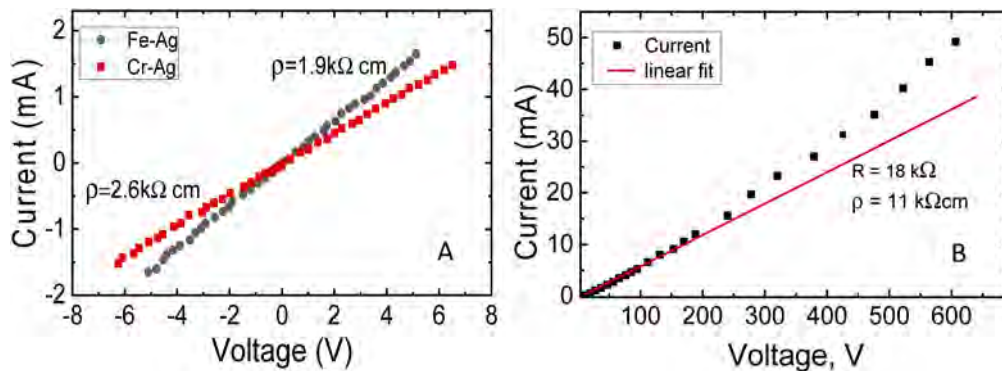
Fig. 2. (A) I-V characteristics of Al:ZnSe with Fe-Ag (circles) and Cr-Ag (squares) contacts; and (B) I-V characteristics of Al:Cr:ZnSe with Indium contacts.

As the voltage increases the electrical current starts to deviate from the linear relationship and exhibits smaller differential resistances. This behavior can be attributed to Joule-heating of

the sample, where more electrons are promoted to the conduction band through the thermionic emission process. A resistivity of 11 kΩcm was estimated, from the straight-line fit < 100 V. Next, the EL and PL characterization of sample #1 was conducted using the experimental setup shown in Fig. 3.
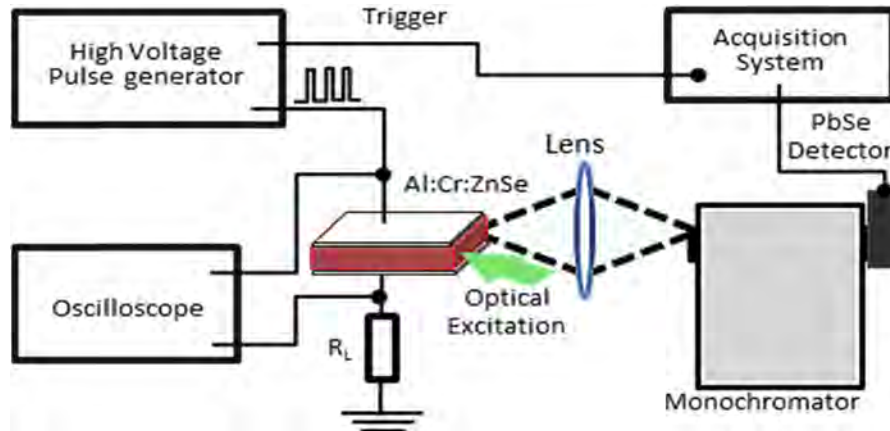
Fig. 3. The experimental setup for EL and PL measurements.

3.   Electroluminescence of Al:Cr:ZnSe

Luminescence from the Cr:Al:ZnSe crystal (sample #1, $N_{Cr} \approx 2 \times 10^{18}$ cm^3) was measured over 1.7-3.0 μm spectral range. Signal, as shown in Fig. 3, was collected using a CaF$_2$ lens into monochromator (Acton Research SpectraPro-300i) with PbSe detector (Thorlabs PDA20H) and measured with the use of a boxcar integrator and an Acton Research data acquisition system. A high-voltage pulse generator (AVTECH AVR-8A-B) was used for electrical excitation with a pulse duration of 200 μs, a repetition rate of 5 Hz, and output voltages of up to 1000 V. The applied voltage and the current through the sample were measured utilizing a load resistor (R$_L$). The photo-emission signal was initially measured directly by PbSe detector with the use of a 2 or a 3 μm long-pass filters. As shown in Fig. 4, (a) square voltage pulse applied across the sample (A) results in a flow of current without significant charging (B) and produces a consistent EL signal (C), which is seen with the 2 μm filter and is completely eliminated by the 3 μm filter. This indicates that the measured signal is consistent with the luminescence band of Cr^{2+} ^{5}T$_2 \rightarrow ^5$E transition. The EL was measured as the applied voltage across the sample was increased. From this measurement, a plot of the EL as function of the calculated current density was made, which follows a linear relationship as can be seen in Fig. 4 – (D). The EL signal was sufficiently strong for the EL spectra measurements using the monochromator. Figure 4. – E depicts comparison of the EL and PL spectra measured under CW 532 nm radiation excitation with close to identical signal collection efficiencies. The measured spectra are in good agreement with each other and with the characteristic Cr^{2+} emission. The amplitude in the EL spectrum is ~25% of the PL spectrum amplitude under 532 nm CW excitation, which has a 100% quantum yield [24]. This indicates a good electrical excitation efficiency. To make a more representative estimation of the EL efficiency the cross-section of electrical excitation was calculated.

The cross-section of electrical excitation was calculated by comparing EL and PL signals measured with identical signal collection geometries. A direct optical excitation of the ^{5}T$_2 \rightarrow ^5$E transition in Cr^{2+} ions was used for PL. Al:Cr:ZnSe crystal (sample #2, $N_{Cr} \approx 2 \times 10^{18}$ cm^3) with a specially cleaved emitting edge, ~2.6×2.6×1 mm^3 dimensions, and a ~54 kΩcm ($N_e \approx 6 \times 10^{11}$ cm^{-3}) resistivity was used in this experiment. For optical excitation 1560 nm radiation of an
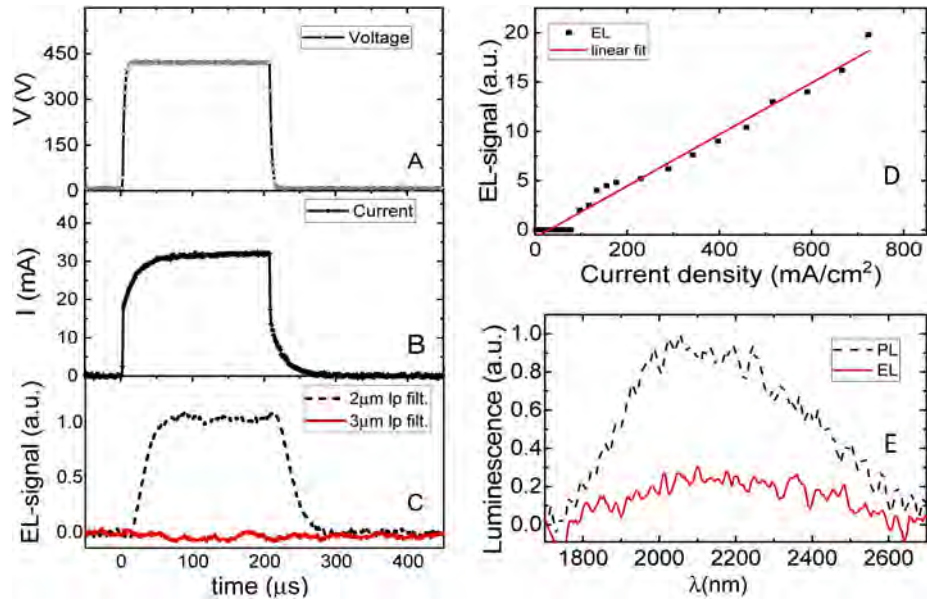
Fig. 4. Oscilloscope traces of voltage (A), current (B), and electroluminescence with 2 (dashed) and 3 μm (solid) long-pass filters (C); Electroluminescence signal as a function of current density (solid squares) and linear fit (solid line) (D) PL spectrum from 100 mW of 532 nm excitation (dashed) and EL spectrum at 900 V applied (solid) (E).

Er:fiber laser (IPG photonics ELR-20-1560-LP) was used, which, as shown in Fig. 1, overlaps with the absorption band of Cr^{2+}. The excitation radiation with intensity 2.8 W/cm^2 was directed on the sample at close to normal incidence. The 78 mV signal was measured by PbSe detector after 2 μm filter. Electrical excitation under 415 V (current density 77 mA/cm^2) applied across the sample, produced, as shown in Fig. 5, (a) signal at 4.5 mV level on the same detection platform.
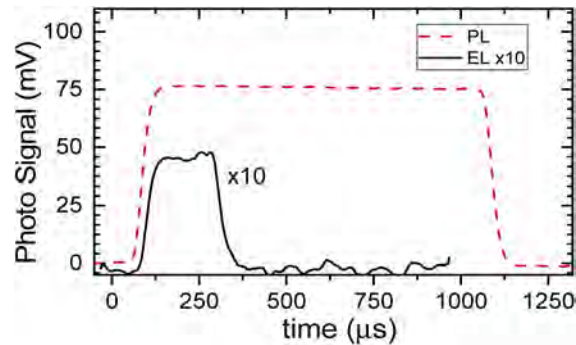
Fig. 5. EL signal at current density of 77 mA/cm^2 (solid) and PL under 2.8 W/cm^2 intensity at 1560 nm (dashed line).

By considering steady-state rate equations for optical and electron impact excitation of Cr and assuming linear dependence of EL on current density, which is reasonable for low-field excitation regime, shown in Fig. 4. - D, the amplitude of photo signal can be approximated as, $S_{(ph;el)} = \phi_{(ph;el)} \cdot \sigma_{(ab; el)}[\eta_{QY} \cdot \eta_{det} \cdot V_{sample} \cdot N_{Cr}]$. Where, $S_{(ph;el)}$ is the EL or PL signal amplitude, $\phi_{(ph;el)}$ is photon or electron flux, $\sigma_{(ab; el)}$ is the cross-section of optical absorption or the cross-section of electrical excitation, η_{QY} is the luminescence quantum yield, η_{det} is the

detector responsivity, V_{sample} is the excited sample volume and N_{Cr} is the Cr^{2+} concentration. Here, the assumptions of a small excitation rate that does not significantly change the chromium concentration at the ground state, and constant photon and electron flux in the crystal were made. The parameters in the brackets are identical for electrical and optical excitations. Making use of the known absorption cross-section at 1560 nm, current density, optical excitation flux, and the measured ratio of the detected signals for optical and electrical excitation, the cross-section of electrical excitation was estimated to be $\sigma_{el} \approx 10^{-18} cm^2$.

Using the estimated cross-section of electrical excitation, the magnitude of the current density required to achieve laser threshold was calculated. The intensity of the optical radiation in our experiment was ~2.8 W/cm^2. This value is ~170 times smaller than the minimum threshold intensity of ~0.5 kW/cm^2 for lasing under optical excitation at a similar wavelength, reported in [25]. Comparing these results with our data a threshold current density of ~0.24 kA/cm^2 would be required to reach the laser threshold in the Al:Cr:ZnSe sample. The cross-section of electrical excitation strongly depends on the electron energy distribution, which is a function of the electric field. At higher fields, the number of electrons possessing enough kinetic energy to excite Cr ions will increase, making ~0.24 kA/cm^2 an upper estimate for the current density threshold. Theoretical modeling of electrical excitation dependence on the electric field in Al:Cr:ZnSe should be done, which is a subject for a separate study. The estimated current density for a laser threshold is smaller than the threshold reported for the first RT CW blue diode based on II-VI semiconductors (1.4 kA/cm^2) [26]. It indicates the feasibility of the development of electrically pumped Cr:ZnSe lasers. Optimization of the electrical conductivity of Al:Cr:ZnSe crystals for laser applications should also take into account free-carrier absorption of n-type Al:ZnSe samples in the mid-IR spectral range [27]. This effect in combination with a strong dependence of the impact cross-section on the electrical field requires utilization of the laser active Cr:ZnSe layers with a relatively small values of conductivity. Therefore, one of the possible structures of the electrically pumped Cr:ZnSe laser should be based on laser active layer with depleted conductivity cladded by layers with high conductivity and small index of refraction. It will help minimize optical losses, increase electrical field and provide wave guiding effect in the active layer.

4. Conclusion

Monocrystalline Cr:ZnSe were n-type doped with Al, resulting in ~50 Ωcm to ~54 kΩcm resistivity. Ohmic contacts were formed based on Cr(Fe)-Ag thin film and Indium "ironing," were used. Both methods yielded reliable Ohmic contacts. Strong EL was obtained in the n-type Al:Cr:ZnSe with resistivities 11 and 54 kΩcm. The cross-section of impact excitation was calculated to be $\sigma_{el} \approx 10^{-18}$ cm^2 based on the comparison of the EL and PL signal strengths. This value is close to the maximum absorption cross-section of Cr^{2+} ions at $^5T_2 \rightarrow ^5E$ laser transition. Calculation of the threshold current density was also performed, indicating ~ 0.24 kA/cm^2 should be sufficient for reaching laser oscillation in the Al:Cr:ZnSe under electrical impact excitation.

Disclosures

The work reported here partially involves intellectual property developed at the University of Alabama at Birmingham (UAB). This intellectual property has been licensed to the IPG Photonics Corporation. Drs. Fedorov and Mirov declare competing financial interests.

References

1. S. Mirov, V. Fedorov, I. Moskalev, D. Martyshkin, and C. Kim, "Progress in Cr^{2+} and Fe^{2+} doped mid-IR laser materials," Laser Photonics Rev. **4**(1), 21–41 (2010).
2. S. B. Mirov, V. V. Fedorov, D. Martyshkin, I. S. Moskalev, M. Mirov, and S. Vasilyev, "Progress in Mid-IR Lasers Based on Cr and Fe-Doped II-VI Chalcogenides," IEEE J. Sel. Top. Quantum Electron. **21**(1), 292–310 (2015).
3. S. B. Mirov, I. S. Moskalev, S. Vasilyev, V. Smolski, V. V. Fedorov, D. Martyshkin, J. Peppers, M. Mirov, A. Dergachev, and V. Gapontsev, "Frontiers of Mid-IR lasers based on transition metal doped chalcogenides," IEEE J. Sel. Top. Quantum Electron. **24**(5), 1–29 (2018).
4. V. V. Fedorov, A. Gallian, I. Moskalev, and S. B. Mirov, "En route to electrically pumped broadly tunable middle infrared lasers based on transition metal doped II-VI semiconductors," J. Lumin. **125**(1-2), 184–195 (2007).
5. B. M. Kimpel, K. Lobet, H. Schulz, and E. Zeitler, "Generation of near-infrared light pulses from ZnS: Cr under laser-enhanced cathode-beam excitation," Meas. Sci. Technol. **9**, 1383–1388 (1995).
6. G. Scamarcio, F. Capasso, A. L. Hutchinson, T. Tanbun-Ek, D. Sivco, and A. Y. Cho, "Narrow-band electroluminescence at 3.5 µm from impact excitation and ionization of Fe2+ ions in InP," Appl. Phys. Lett. **68**(10), 1374–1376 (1996).
7. L. Luke, V. V Fedorov, I. Moskalev, A. Gallian, and S. B. Mirov, "Middle-infrared electroluminescence of n-type Cr doped ZnSe crystals," Proc. SPIE **6100**, 61000Y (2006).
8. J. Jaeck, R. Haidar, E. Rosencher, M. Caes, M. Tauvy, S. Collin, N. Bardou, J. L. Pelouard, F. Pardo, and P. Lemasson, "Room-temperature electroluminescence in the mid-infrared (2-3 (m) from bulk chromium-doped ZnSe," Opt. Lett. **31**(23), 3501–3503 (2006).
9. J. Jaeck, R. Haidar, F. Pardo, J. L. Pelouard, and E. Rosencher, "Electrically enhanced infrared photoluminescence in Cr:ZnSe," AIP Conf. Proc. **96**(21), 211107 (2010).
10. N. A. Vlasenko, P. F. Oleksenko, M. A. Mukhlyo, L. I. Veligura, and Z. L. Denisova, "Stimulated emission of Cr^{2+} ions in ZnS: Cr thin-film electroluminescent structures," Fiz. Napivprovidn., Kvantova Optoelektron. **12**(4), 362–365 (2009).
11. A. Burger, K. Chattopadhyay, J. O. Ndap, X. Ma, S. H. Morgan, C. I. Rablau, C. H. Su, S. Feth, R. H. Page, K. I. Schaffers, and S. A. Payne, "Preparation conditions of chromium doped ZnSe and their infrared luminescence properties," J. Cryst. Growth **225**(2-4), 249–256 (2001).
12. J. C. Bouley, P. Blanconnier, A. Herman, P. Ged, P. Henoc, and J. P. Noblanc, "Luminescence in highly conductive n-type ZnSe," J. Appl. Phys. **46**(8), 3549–3555 (1975).
13. M. Aven, "Diffusion of Aluminum in the ZnSe[Single Bond]ZnTe System," J. Appl. Phys. **41**(5), 1930–1934 (1970).
14. H. Takenoshita, K. Kido, and K. Sawai, "Cathodoluminescence study on diffusion coefficients of Al, Ga and In in ZnSe," Jpn. J. Appl. Phys. **25**(Part 1, No. 10), 1610–1611 (1986).
15. G. N. Ivanova, D. D. Nedeoglo, N. D. Negeoglo, V. P. Sirkeli, I. M. Tiginyanu, and V. V. Ursaki, "Interaction of intrinsic defects with impurities in Al doped ZnSe single crystals," J. Appl. Phys. **101**(6), 063543 (2007).
16. Y. Namikawa, S. Fujiwara, and T. Kotani, "A1 diffused conductive ZnSe substrates grown by physical vapor transport method," J. Cryst. Growth **229**(1-4), 92–97 (2001).
17. O. Gafarov, A. Martinez, V. Fedorov, and S. Mirov, "Enhancement of Cr and Fe diffusion in ZnSe/S laser crystals via annealing in vapors of Zn and hot isostatic pressing," Opt. Mater. Express **7**(1), 25 (2017).
18. M. Prokesch, K. Irmscher, J. Gebauer, and R. Krause-Rehberg, "Reversible conductivity control and quantitative identification of compensating defects in ZnSe bulk crystals," J. Cryst. Growth **214-215**, 988–992 (2000).
19. M. Aven and H. H. Woodbury, "Purification of II-VI compounds by solvent extraction," Appl. Phys. Lett. **1**(3), 53–54 (1962).
20. F. Xu, M. Vos, and J. H. Weaver, "Schottky-barrier at Au/ZnSe(100) interfaces," Phys. Rev. **38**(18), 418–421 (1988).
21. S. Kasap and P. Copper, *Springer Handbook of Electronic and Photonic Materials* (Springer, 2017), pp. 365–383.
22. T. Drummond, "Work Functions of the transition metals and metal silicides," 1–24 (1999).
23. R. G. Kaufman and P. Dowbor, "Mechanism of formation of Ohmic contacts to ZnSe, ZnS, and mixed crystals $ZnSXSe_{1-X}$," J. Appl. Phys. **45**(10), 4487–4490 (1974).
24. J. M. Peppers, V. V Fedorov, and S. B. Mirov, "Spectroscopic characterization of Cr^{2+} ions in ZnSe / ZnS crystals under visible excitation," Proc. SPIE **9342**, 1–6 (2015).
25. I. T. Sorokina, E. Sorokin, S. Mirov, V. Fedorov, V. Badikov, V. Panyutin, A. Di Lieto, and M. Tonelli, "Continuous-wave tunable Cr^{2+}ZnS laser," Appl. Phys. B: Lasers Opt. **74**(6), 607–611 (2002).
26. N. Nakayama, S. Itoh, T. Ohata, K. Nakano, H. Okuyama, M. Ozawa, A. Ishibashi, M. Ikeda, and Y. Mori, "Room temperature continuous operation of blue-green laser diodes," Electron. Lett. **29**(16), 1488–1489 (1993).
27. B. V. Dutt, O. K. Kim, and W. G. Spitzer, "Free-carrier absorption of n -type ZnSe: Al," J. Appl. Phys. **48**(5), 2110–2111 (1977).